Heating-Induced Micelle to Vesicle Transition in the Cationic−Anionic Surfactant Systems: Comprehensive Study and Understanding

Haiqing Yin,[†] Jianbin Huang,*[,†] Yiyang Lin,[†] Yongyi Zhang,[†] Shunchen Qiu,[†] and Jianping Ye[‡]

State Key Laboratory for Structural Chemistry of Unstable and Stable Species, College of Chemistry and Molecular Engineering, Peking University, Beijing, 100871, People's Republic of China and Institute of Chemistry, Chinese Academy of Science, Beijing, People's Republic of China

Received: October 23, 2004; In Final Form: January 6, 2005

Heating-induced micelle to vesicle transition (MVT), which has been rarely reported in surfactant systems, was systemically studied in a number of mixed cationic−anionic surfactant systems. According to the turbidity measurements, the investigated systems can be divided into two classes: Class A and B. Heating-induced MVT was observed in Class A at certain total surfactant concentrations and mixed surfactant ratios, while no such transition was found in Class B. Further investigations revealed that the heating-induced MVT is more likely to take place in the cationic−anionic surfactant systems with relatively stronger molecule interaction and larger micelle aggregation number. The effects of several physicochemical factors, such as the variation of mixed surfactant ratios and the addition of *n*-decanol on the heating-induced MVT, were also studied.

Introduction

Amphiphilic molecules have the ability to form various organized assemblies in solutions such as spherical micelles, cylindrical micelles, vesicles, or more complex structures, i.e., bicontinuous phases and lyotropic liquid crystals, etc. These self-assemblies have been widely exploited in diverse areas such as catalysis, biochemistry, and material synthesis as well as petroleum, chemical, and pharmaceutical industries.[1] In the past few decades research on the formations and transformations of different self-assemblies has been investigated in numerous works,[2] especially on the effect of cosurfactants' addition, pH, temperature, salts, force fields, etc.

Compared with other methods, temperature variation can provide a quite simple way in tailoring assemblies, which has attracted special attention of scientists.[3] The temperature-sensitive systems are convenient for studying the individual stage of the aggregate transition since the transition can be cycled or stopped at any required step in measurements. Kinetic aspects can also be examined by controlling the heating and cooling rates.

It is known that temperature has great effect on the nonionic surfactant systems. Usually such systems have cloud point properties i.e., heating-induced phase separations,[4] which are attributed to the dehydration of the hydrophilic groups of surfactants upon heating. In contrast, in ionic surfactant systems the aggregate size normally decreases when the temperature increases.[5] In fact, in most vesicular systems phase transitions[6] or transitions from vesicle to micelle[7] usually take place with increasing temperature. However, the reverse process, such as heating-induced micelle to vesicle transition (MVT), has been rarely been reported in surfactant systems. It was once observed by H. Hoffmann in some nonionic surfactant systems[8] and mixed ionic surfactant/cosurfactant systems,[9] which was attributed to the dehydration of the surfactant headgroup. Recently, heating-induced MVT was also studied in mixed lipid/ionic surfactant systems.[10] The decreasing solubilization ability of surfactants in lipid vesicles upon heating was considered to account for the transition. In our previous study we reported a heating-induced MVT in the mixed cationic−anionic surfactant system of sodium *n*-dodecyl sulfate (SDS)/*n*-dodecyltriethylammonium bromide (DTEAB).[11] Afterward, we also observed similar transitions in some other cationic−anionic surfactant systems. Nevertheless, the transitions in our cases cannot be simply explained with the interpretations for the systems mentioned above and may have a more complex origin. Hence, it is necessary to perform comprehensive studies on the heating-induced MVT in the cationic−anionic surfactant systems.

In this work heating-induced MVT was investigated extensively in a number of cationic−anionic surfactant systems. It was revealed this transition may be a general phenomenon in the cationic−anionic surfactant systems with relatively stronger molecule interaction and larger micelle aggregation number. On this basis the transition was adjusted by several physicochemical factors, such as the mixed surfactant ratio and addition of *n*-decanol.

Experimental Section

Materials. Quaternary ammonium bromides including *n*-dodecylmethyldiethylammonium bromide (DME_2AB), *n*-dodecyltriethylammonium bromide (DTEAB), *n*-dodecyltripropylammonium bromide (DTPAB), and *n*-decyltriethylammonium bromide (DeTEAB) were prepared by reaction of 1-bromododecane and the corresponding trialkylamine. Sodium laurate (SL) was prepared by neutralizing lauric acid with NaOH in ethanol. Sodium *n*-decyl sulfate (SDeS), sodium *n*-octylsulfonate (SOS), and sodium *n*-dodecylsulfonate ($SDSO_3$) were products of Beijing Chemical Co. Sodium *n*-dodecyl sulfate (SDS) and sodium *n*-dodecylbenzenesulfonate (SDBS) were bought from ACROS ORGANICS Co. All the surfactants were

* To whom correspondence should be addressed. Phone: 86-10-62753557. Fax: 86-10-62751708. E-mail: JBHuang@pku.edu.cn.
† Peking University.
‡ Chinese Academy of Science.

10.1021/jp045158a CCC: $30.25
Published on Web 02/12/2005

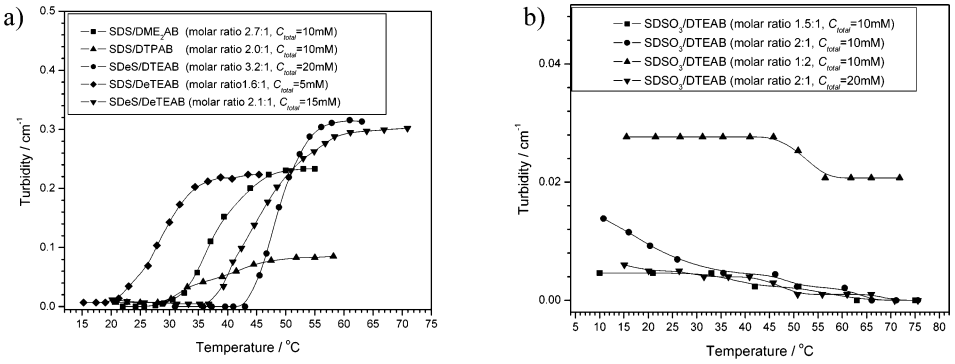

Figure 1. Turbidity heating curves for some Class A (a) and Class B (b) systems.

recrystallized five times from mixed solvents of ethanol−acetone or ether−acetone. The purity of the surfactant was examined, and no surface tension minimum was found in the surface tension curve. The water used was redistilled from potassium permanganate. The other reagents were products of A. R. Grade.

Turbidity Measurements. Turbidity measurements were carried out with a Shimadzu UV-250 spectrophotometer at 514.5 nm.

DLS Measurements. Dynamic light scattering measurements were performed with a spectrometer (ALV-5000/E/WIN Multiple Tau Digital Correlator) and a Spectra-Physics 2017 200 mW Ar laser (514.5 nm wavelength). The scattering angle was 90°. The intensity autocorrelation functions were analyzed using the Contin method, and the apparent hydrodynamic radius $<R_h>$ was deduced from the diffusion coefficient D by the Stokes−Einstein formula $R_h = k_B T/(6\pi\eta D)$.

Transmission Electron Microscopy. Samples for TEM were prepared by negative-staining technique with uranyl acetate water solution. A JEM-100CX electron microscope was employed in the microscopic observation.

Rheology Measurements. The rheological properties of samples were measured with a ThermoHaake RS300 rheometer. A double-gap cylinder sensor system was used with an outside gap of 0.30 mm and an inside gap of 0.25 mm.

DSC Measurements. Differential canning calorimetry measurements were carried out (1 °C/min) using a Micro DCS III (Setaram-France) instrument.

Time-Resolved Fluorescence Quenching (TRFQ). This method was applied to determine the micelle aggregation number (N) of the micellar system using pyrene as a fluorescence probe and dodecylpyridinium chloride as a quencher of the fluorescence probe. Pyrene fluorescence decay curves were monitored by a Horiba NAES-1100 single-photon counting spectrophotometer (excitation at 337 nm and emission at 394 nm).

Calculation of Micelle Aggregation Number. The fluorescence decay eqs 1 and 2 in the absence and presence of quencher, respectively, are fitted using a weighted least-squares[12] procedure by a DECAN 1.0 software

$$I(t) = I(0)\exp(-t/\tau) \quad (1)$$

$$I(t) = I(0)\exp\{-A_2 t - A_3[1 - \exp(-A_4 t)]\} \quad (2)$$

where $I(t)$ and $I(0)$ are the fluorescence intensities at time t and time zero, respectively, τ is the pyrene fluorescence lifetime and A_2, A_3, and A_4 are the time-independent fitting parameters. The micelle aggregation number N is obtained by eq 3

$$N = A_3[(C - \mathrm{cmc})/[Q][1 + (A_2 - 1/\tau)/A_3 A_4]^2 \quad (3)$$

where C is the total surfactant concentration, cmc is the critical micelle concentration, and $[Q]$ is the concentration of quencher.

Critical Micelle Concentration Measurements. The critical micelle concentrations of surfactants in aqueous solutions were obtained from the surface tension vs concentration curves by the drop volume method. The ionic strength of the system was adjusted to 0.1 mol $kg^{-1}$with NaBr all through the measurements.

β **Parameter**. On the basis of the regular solution theory, interaction parameters between surfactant molecules in micelles of mixed systems (named as β_m) are obtained from critical micelle concentration data using eqs 4 and 5[13]

$$\frac{(X_1^{\mathrm{M}})^2 \ln(\alpha_1 C_{12}^{\mathrm{M}}/X_1^{\mathrm{M}} C_1^{\mathrm{M}})}{(1 - X_1^{\mathrm{M}})^2 \ln[(1 - \alpha_1) C_{12}^{\mathrm{M}}/(1 - X_1^{\mathrm{M}}) C_2^{\mathrm{M}}]} = 1 \quad (4)$$

$$\beta_m = \frac{\ln(\alpha_1 C_{12}^{\mathrm{M}}/X_1^{\mathrm{M}} C_1^{\mathrm{M}})}{(1 - X_1^{\mathrm{M}})^2} \quad (5)$$

where X_1^{M} is the mole fraction of surfactant 1 of the total surfactants in the mixed micelle. C_1^{M}, C_2^{M}, and C_{12}^{M} are the critical micelle concentrations for surfactant 1, surfactant 2, and their mixture, respectively, at the mole fraction α_1. The ionic strength of the system was kept constant to avoid the electrical effect.

Results and Discussion

Classification of the Cationic−Anionic Surfactant Systems According to the Turbidity Measurements. Eleven kinds of cationic−anionic surfactant systems were selected for our studies (see the Experimental Section for the full names of the individual surfactants), considering the variation of cationic surfactant headgroups (SDS/DME_2AB, SDS/DTEAB, SDS/DTPAB), anionic surfactant headgroups (SL/DTEAB at pH = 9.2 and 13, respectively, $SDSO_3$/DTEAB, SDBS/DTEAB), as well as the changes of the hydrocarbon chain lengths (SDS/DeTEAB, SDeS/DTEAB, SDeS/DeTEAB, SOS/DTEAB). Turbidity measurements were carried out to monitor the variations upon increasing temperature in all selected systems. According to the turbidity curves, these systems can be divided into two classes which are named as Class A and B. The SDS/DME_2AB, SDS/DTEAB, SDS/DTPAB, SDeS/DTEAB, SDS/DeTEAB, and SDeS/DeTEAB systems belong to Class A, while the SL/DTEAB (pH = 9.2), SL/DTEAB (pH = 13), $SDSO_3$/DTEAB, SDBS/DTEAB, and SOS/DTEAB systems belong to Class B. For Class A there was an obvious increase of the turbidity upon increasing temperature (Figure 1a). During this process the original transparent ap-

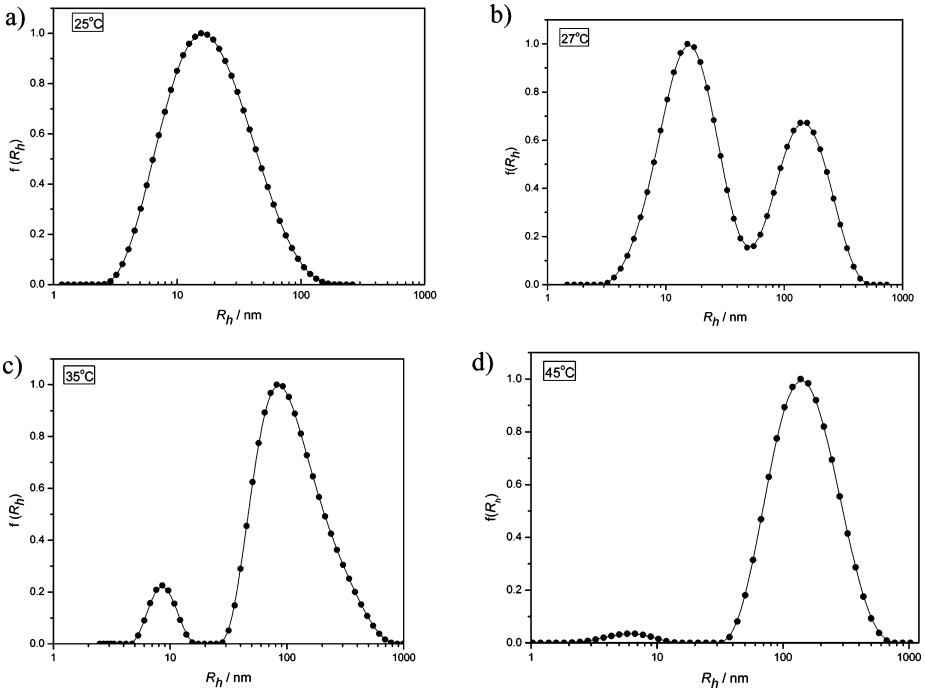

Figure 2. Hydrodynamic radius (R_h) distributions of SDS/DME_2AB (2.7:1, C_{total} = 10 mM) at 25 (a), 27 (b), 35 (c), and 45 °C (d) calculated by the Contin method.

pearance of the solution turned slightly bluish. In contrast, no significant increase of the turbidity upon heating was observed for Class B no matter how the total concentration (C_{total}) or mixed surfactant molar ratio was varied (Figure 1b). The increase of the turbidity with increasing temperature in Class A indicates the size growth or even structural transition of surfactant aggregates, showing a quite different behavior from Class B. Further investigations were performed in the SDS/DME_2AB system selected from Class A to confirm our speculation. In addition, the mixed systems $SDSO_3$/DTEAB and SL/DTEAB (pH = 13), in which the individual surfactants have almost the same hydrocarbon chain length, were also selected from Class B for comparison.

Microstructure Transition upon Temperature Increasing in Class A. From Figure 1a it was found that the temperature interval of obvious turbidity increase for the SDS/DME_2AB system (molar ratio 2.7:1, C_{total} = 10 mM) was from ca. 27 to 45 °C. The average hydrodynamic radius $<R_h>$ was 18 nm at 25 °C measured by DLS (Figure 2a), which is a typical value for a micellar system. The steady rheology measurements clearly revealed the non-Newtonian nature of the solution. As shown in Figure 3, shear-thickening and shear-thinning behaviors took place successively with the increase of shear rate, suggesting the existence of asymmetrical aggregates. Similar rheological behaviors were also reported in some dilute surfactant solutions containing cylindrical micelles.[14] In addition, the average micelle aggregation number ($\langle N \rangle$) is about 1100, calculated from the TRFQ data (see the Experimental Section), showing a typical value of cylindrical micelles.[15] Moreover, TEM results showed that very few small spherical vesicles exist in this system. Hence, it may be concluded that cylindrical micelles are the dominating surfactant aggregates at 25 °C.

However, the situation was different as the temperature increased to 27 °C. DLS plot (Figure 2b) showed that at 27 °C the peak corresponding to the cylindrical micelles shrank compared with that of 25 °C whereas another peak appeared

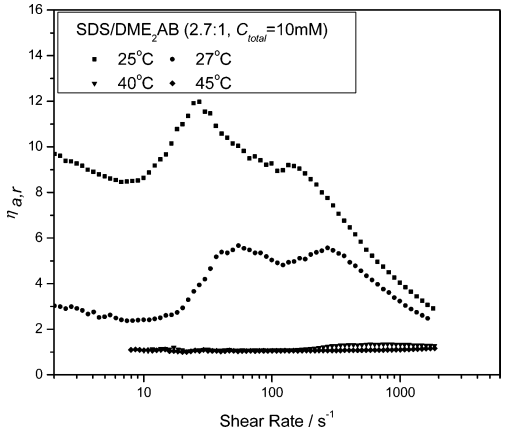

Figure 3. Steady flow curves (apparent relative viscosity $\eta_{a,r}$ vs shear rate) of the system SDS:DME_2AB (2.7:1, C_{total} = 10 mM) at different temperatures ($\eta_{a,r} = \eta/\eta_0$, where η and η_0 are the viscosities of the solution and water, respectively).

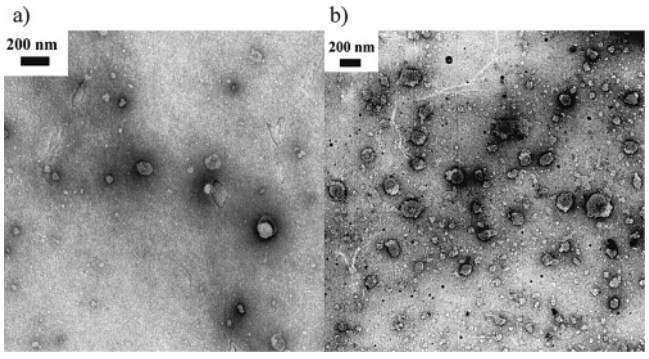

Figure 4. Micrographs of the system SDS/DME_2AB (2.7:1, C_{total} = 10 mM) at 27 (a) and 45 °C (b) by negative-staining technique.

($R_h \approx$ 100 nm). Correspondingly, the formation of spherical vesicles with a diameter of ca. 100−200 nm was observed by TEM (Figure 4a), which coincided with the new peak in the DLS plot. Moreover, there was an obvious decrease of the

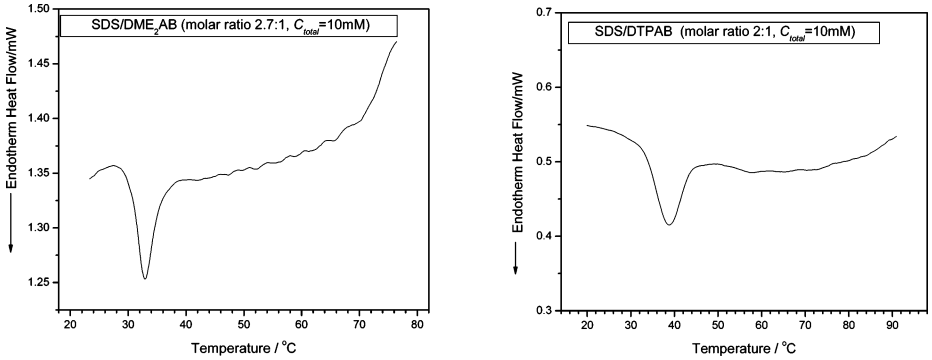

Figure 5. DSC curves of the systems: SDS/DME_2AB system (2.7:1, C_{total} = 10 mM) (a) and SDS/DTPAB (2:1, C_{total} = 10 mM) (b).

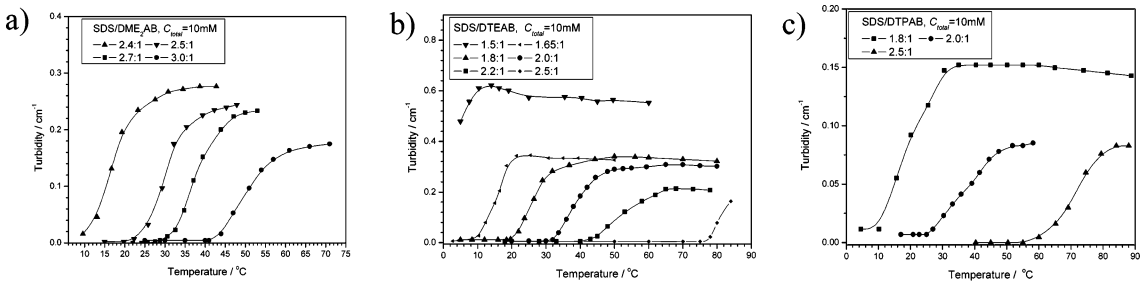

Figure 6. Turbidity heating curves of SDS/DME_2AB (C_{total} = 10 mM) (a), SDS/DTEAB (C_{total} = 10 mM) (b), and SDS/DTPAB (C_{total} = 10 mM) (c) with different mixed surfactant molar ratios.

TABLE 1: List of T_{MVT} for Several Class A Systems

systems	T_{MVT} (°C)
SDS/DME_2AB (2.7:1,C_{total} = 10 mM)	27
SDS/DTPAB (2:1, C_{total} = 10 mM)	30
SDeS/DeTEAB (2.1:1, C_{total} = 15 mM)	37
SDeS/DTEAB (3.2:1, C_{total} = 20 mM)	43
SDS/DeTEAB (1.6:1, C_{total} = 5 mM)	20

TABLE 2: β Parameters in Micelle (β_m) of Several Class A and Class B Systems

systems[a]	β_m
Class A	
SDS/DME_2AB (molar ratio 2.7:1)	−15.0
SDS/DTEAB (molar ratio 2:1)	−13.3
SDS/DTPAB (molar ratio 2:1)	−15.0
Class B	
$SDSO_3$[b]/DTEAB (molar ratio 1:1)	−9.6
SDBS/DEAB (molar ratio 1:1)	−8.9
SL/DTEAB (molar ratio 1:1, pH = 13)	−8.9
SL/DTEAB (molar ratio 1:1, pH = 9.2)	−6.2

[a] T = 25 °C, I (ionic strength) = 0.1 mol.kg^{-1} for all systems if without further notation. [b] cmc of $SDSO_3$ at 40 °C was used due to the limit of the Krafft point.

apparent relative viscosity $\eta_{a,r}$ of the solution at low shear rate (Figure 3), indicating that the shape of aggregates turned from asymmetric to symmetric. All these results suggest the transition from cylindrical micelles to spherical vesicles in the system. Hence, the first turning point of the turbidity heating curve may be considered as the beginning of obvious MVT, and the corresponding temperature will be called T_{MVT}. The T_{MVT}s of several Class A systems are listed in Table 1.

The transition from micelle to vesicle continued as the temperature continued increasing. At 45 °C the system became a complete Newtonian fluid (Figure 3) and the peak assigned to cylindrical micelles almost disappeared in the DLS plot, leaving the peak assigned to vesicles (Figure 2d). Combined with the TEM observation (Figure 4b) it may be concluded that spherical vesicles became the dominating aggregates at 45 °C. Thus, the micelle to vesicle transition upon temperature increasing from 27 to 45°C was demonstrated in the SDS/DME_2AB system (2.7:1, C_{total} = 10 mM), which is coincident with the turbidity measurement result (Figure 1a).

TABLE 3: Average Aggregation Numbers $\langle N \rangle$ of Class A and Class B Systems at 25 °C

systems	$\langle N \rangle$
Class A	
SDS/DME_2AB (2.7:1,C_{total} = 10 mM)	1100
SDS/DTEAB (2:1, C_{total} = 10 mM)	850
SDS/DTPAB (2:1, C_{total} = 10 mM)	430
Class B	
$SDSO_3$/DTEAB (2:1, C_{total} = 10 mM)	188
SL/DTEAB (2:1, C_{total} = 10 mM, pH = 13)	187
SL/DTEAB (2:1, C_{total} = 10 mM, pH = 9.2)	134

Similar rheology, DLS, and TEM results were also obtained in the SDS/DTPAB system (see Figures 1 and 2 in the Supporting Information) and other Class A systems. Referring to our previous work in the SDS/DTEAB system,[11] it can be concluded that the increase of the turbidity upon heating for Class A (Figure 1a) is attributed to the temperature-induced MVT in this kind of systems.

DSC measurements were employed to study the heat effect of the temperature-induced MVT in the Class A systems (Figure 5). Endothermic peaks can be obviously observed in the DSC heating curves. The temperatures for the corresponding peaks coincided with the temperature intervals of MVT obtained from the turbidity measurements. Considering the spontaneity of the transition in these systems, it is demonstrated that the temperature-induced MVT in Class A is accompanied by an increase of entropy.

Turbidity variations of Class A systems during a heating−cooling circulation were also studied (see Figure 3 in the

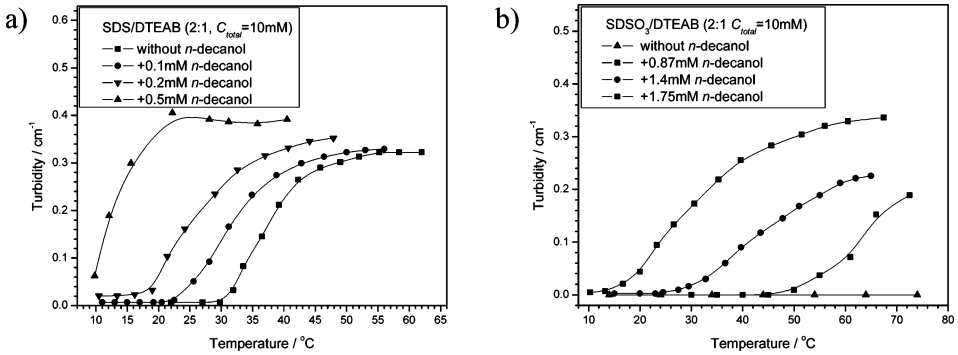

Figure 7. Turbidity variations as a function of temperature for the systems: SDS/DTEAB (2:1, C_{total} = 10 mM) (a) and $SDSO_3$/DTEAB (2:1, C_{total} = 10 mM) (b) upon addition of *n*-decanol.

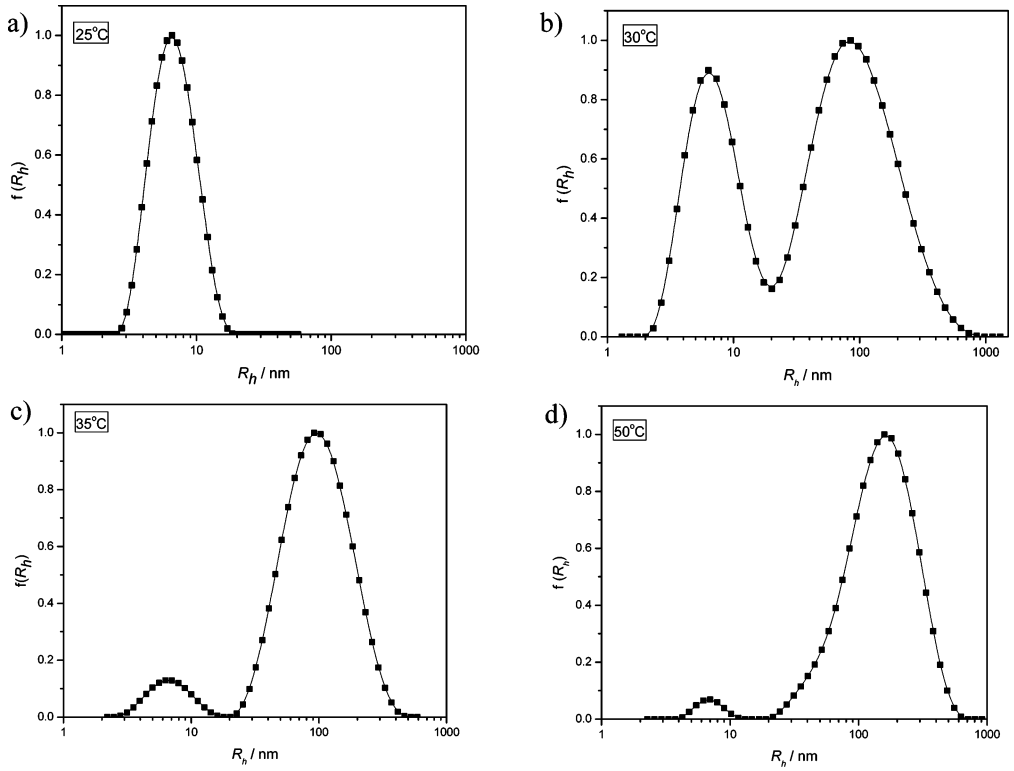

Figure 8. R_h distributions of $SDSO_3$/DTEAB (2:1, C_{total} = 10 mM) upon addition of 1.4 mM *n*-decanol at 25 (a), 30 (b), 35 (c), and 50 °C (d).

Supporting Information). The shapes of the cooling curves are similar to the heating curves, although they do not overlap completely. In addition, all systems can recover their original states after the heating−cooling circulation, suggesting the temperature-induced MVT in these systems may be considered as a reversible process.

Effect of Temperature on Class B. As mentioned above, no increase of turbidity upon heating was observed for Class B. From the results of DLS, the size of micelles of Class B always decreased with increasing temperature (see Figure 4 in the Supporting Information), which is similar to the behavior of a single ionic surfactant system. The results of DLS and TEM also showed no vesicle formation upon heating in these systems. Additionally, no obvious heat effect was detected by DSC measurements.

In conclusion, heating-induced MVT was demonstrated in Class A while no such transition was found in Class B. Considering the complexity of rheology, DLS, as well as TEM and the coincidence of these results with the turbidity measurements, the increase of turbidity upon heating may be used as an easy and effective way to find temperature-induced MVT in the cationic−anionic surfactant systems.

Differences of Molecule Interaction and Micelle Aggregation Number between Class A and B. The nature of formation or transformation of self-assemblies in solutions is to satisfy the corresponding requirements of energy and geometry. Therefore, the interaction between the surfactant molecules in the organized assemblies should play an important role for the heating-induced MVT in our systems. On the basis of regular solution theory, the β parameter is utilized to estimate the molecule interaction in mixed systems.[13] The β parameters in micelles (β_m) of several Class A and B systems have been calculated (see Experimental Section) and listed in Table 2. From Table 2 it is found that β_m parameters of all the studied systems are negative, indicating the existence of an attractive interaction between the surfactant molecules. Among these systems the absolute value of the β_m parameter of Class A is above 13 while that of Class B is below 10. It is worth noting that β_m parameters of Class A are generally more

negative than those of Class B, indicating stronger interaction between the surfactant molecules in Class A.[13]

The average micelle aggregation numbers ($\langle N \rangle$) of several Class A and B systems have been also measured and listed in Table 3. It is clearly shown that Class A has a larger $\langle N \rangle$ than Class B. Combined with the results of DLS, it may be concluded that surfactant molecules pack more closely and aggregate into larger micelles in Class A.

The critical packing parameter p proposed by Israelachvili et al.[16] has been widely used to explain the formation and transformation of self-assemblies in dilute surfactant solutions:[17] $0 \leq p \leq 1/3$ for sphere micelle, $1/3 \leq p \leq 1/2$ for cylinder micelle, and $1/2 \leq p \leq 1$ for bilayer structure (p is defined as $v/a_0 l_c$, where v is the surfactant tail volume, l_c is the tail length, and a_0 is the equilibrium area per molecule at the aggregate surface). Considering the fact that the individual surfactant molecules of the Class A and B systems in Table 3 have the same length of hydrocarbon chain, v/l_c is almost the same and the variation of a_0 will significantly influence the p values of these systems. The results of β_m and $\langle N \rangle$ suggest that Class A systems have relatively larger p values than Class B systems, which may be closer to the case of vesicle formation. Thus, the micelles of Class A are more easily transformed into vesicles than those of Class B. Furthermore, the strong attraction between oppositely charged surfactant headgroups of Class A systems may also impart some nonionic character to the mixed micelles,[18] which will cause a_0 to be effectively decreased upon heating due to dehydration of headgroups. Hence, the transformation from micelles to vesicles may occur as the temperature increases beyond a certain value (T_{MVT}). As for Class B, the size of micelles will generally decrease upon heating no matter how the total concentration or mixed surfactant ratio is varied, showing similar behavior in ionic surfactant systems. Thus, it can be concluded that heating-induced MVT is more likely to take place in the cationic−anionic surfactant systems with a relatively stronger molecule interaction and larger micelle aggregation number. On this basis the effects of several physicochemical factors on the heating-induced MVT, such as variation of mixed surfactant ratios and addition of *n*-decanol, were further studied.

Variation of the Mixed Surfactant Molar Ratio in Class A. Figure 6 reveals that the heating-induced MVT in Class A has a strong dependence on the mixed surfactant molar ratio. T_{MVT} decreased obviously with the mixed ratio approaching 1:1. It is known that the electrostatic attraction between the headgroups of oppositely charged surfactants in cationic−anionic surfactant systems becomes stronger as the mixed ratio approaches equimolar, which will make the surfactant molecules pack closer in the aggregates. Correspondingly, the p value of the system will increase and be closer to the case of vesicle formation.[19] DLS results also demonstrated the formation of larger aggregates in Class A systems as the mixed ratio approached 1:1 (see Figure 5 in the Supporting Information). Therefore, MVT will take place at a lower temperature as the mixed ratio approaches equimolar.

Addition of *n*-Decanol. Recently, much interest has been focused upon the addition of cosurfactants such as medium-chained alcohols in surfactant solutions for their great impact on the formation and transformation of surfactant self-assemblies.[20] Due to the poor solubility in water, medium-chained alcohols are considered to solubilize into the palisade of micelles with the hydroxyl groups toward the surface,[21] which can cause an increase of the p value and growth of micelles. Combined with our previous discussion, it can be expected that the addition of medium chained alcohols may facilitate heating-induced MVT and reduce the T_{MVT} of Class A systems. In fact, the addition of a tiny amount of *n*-decanol effectively lowered the T_{MVT} of the SDS/DTEAB system (Figure 7a).

Furthermore, it is interesting to find that as *n*-decanol was added into some Class B systems such as $SDSO_3$/DTEAB (2:1, $C_{total} = 10$ mM), the micelles of the system were transformed into vesicles upon increasing temperature, which was demonstrated by the turbidity (Figure 7b) and DLS (Figure 8) measurements. TRFQ data also revealed that $\langle N \rangle$ of the system $SDSO_3$/DTEAB (2:1, $C_{total} = 10$ mM) increased from 188 to 432 at 25 °C (close to the case of Class A) after addition of 1.4 mM *n*-decanol, indicating a notable increase of the p value of the system. Hence, addition of *n*-decanol may promote the occurrence of heating-induced MVT in this case.

Conclusion

Heating-induced MVT was systemically investigated in a number of cationic−anionic surfactant systems. Turbidity measurements can be used as an easy and effective way to determine the occurrence of MVT in the cationic−anionic surfactant systems. It is predicted that heating-induced MVT will take place more easily in the cationic−anionic surfactant systems with relatively stronger molecule interactions and larger micelle aggregation numbers. On this basis T_{MVT} can be efficiently adjusted by variation of the mixed surfactant ratios or addition of *n*-decanol. It is also noteworthy that the addition of *n*-decanol can promote the occurrence of heating-induced MVT in some cationic−anionic systems in which no such transition is observed before addition of *n*-decanol. We hope this work may advance the understanding of the temperature-induced self-assembly transitions and promote its applications in related fields.

Acknowledgment. This work was supported by National Natural Science Foundation of China (20233010, 20373003, 20425310).

Supporting Information Available: Rheology, DLS, and TEM results for the SDS/DTPAB system (Figures 1, and 2), turbidity variations of Class A systems (Figure 3), rheology variations for the $SDSO_3$/DTEAB and SL/DTEAB systems, and rheology variations for the SDS/DTEAB and SDS/DTPAB systems. This material is available free of charge via the Internet at http://pubs.acs.org.

References and Notes

(1) (a) Evans, D. F.; Wennerstrom, H. *The Colloidal Domain, Where Physics, Chemistry, Biology, and Technology Meet*, 2nd ed.; John Wiley: New York, 1999. (b) Birdi, K. S. *Surface and Colloid Chemistry*; CRC Press: New York, 1997. (c) Fendler, J. H. *Membrane Mimetic Chemistry*; John Wiley: New York, 1982. (d) Rosoff, M. *Vesicles*; Marcel Dekker: New York, 1996. (e) Makai, A.; Csanyi, E.; Nemeth, Z.; Palinkas, J.; Eros, I. *Int. J. Pharm.* **2003**, *256*, 95−107. (f) Kresge, C. T.; Leonowicz, M. E.; Roth, W. J.; Vartuli, J. C.; Beck, J. S. *Nature* **1992**, *359*, 710−712.

(2) (a) Hao, J. C.; Hoffmann, H.; Horbaschek, K. *J. Phys. Chem. B* **2000**, *104*, 10144−10153. (b) Hassan, P. A.; Raghavan, S. R.; Kaler, E. W. *Langmuir* **2002**, *18*, 2543−2548. (c) Mao, M.; Huang, J. B.; Zhu, B. Y.; Ye, J. P. *J. Phys. Chem. B* **2002**, *106*, 219−225. (d) Wang, C. Z.; Huang, J. B.; Tang, S. H.; Zhu, B. Y. *Langmuir* **2001**, *17*, 6389−6392.

(3) (a) Bott, R.; Wolff, T.; Zierold, K. *Langmuir* **2002**, *18*, 2004−2012. (b) Gorski, N.; Kalus, J. *Langmuir* **2001**, *17*, 4211−4215. (c) Kumar, S.; Sharma, D.; Khan, Z. A.; Din, K. U. *Langmuir* **2001**, *17*, 5813−5816. (d) Forster, S.; Plantenberg, T. *Angew. Chem., Int. Ed.* **2002**, *41*, 688−714.

(4) (a) Robson, R. J.; Dennis, E. A. *J. Phys. Chem.* **1977**, *81*, 1075. (b) Corti, M.; Minero, C.; Degiorgio, V. *J. Phys. Chem.* **1984**, *88*, 309. (c) Ravey, J. C. *J. Colloid Interface Sci.* **1983**, *94*, 289. (d) Hayter, J. B.; Zulauf, M. *Colloid Polym. Sci.* **1982**, *260*, 1023.

(5) (a) Mazer, N. A.; Benedek, G. B.; Carey, M. C. *J. Phys. Chem.* **1980**, *84*, 3105. (b) Porte, G.; Appell, J.; Poggl, Y. *J. Phys. Chem.* **1980**, *84*, 3105. (c) Yu, Z. J.; Zhao, G. X. *J. Colloid Interface Sci.* **1989**, 414−420. (d) Rohde, A.; Sackmann, E. *J. Colloid Interface Sci.* **1979**, *70*, 494.

(6) (a) Ueno, M.; Katoh, S.; Kobayashi, S.; Tomoyama, S.; Obata, R.; Nakao, H.; Ohsawa, S.; Koyama, N.; Morita, Y. *Langmuir* **1991**, *7*, 918−922. (b) Chapman, D.; Williams, R. M.; Ladbrooke, B. D. *Chem. Phys. Lipids* **1967**, *1*, 445. (c) Chapman, D. *Form and Function of Phospholipids*; Ansell, G. B., Hawthorne, J. N., Eds.; Elsevier: Amsterdam, 1973; p 117. (d) Wikinson, D. A.; Nagle, J. F. *Liposomes*; Knight, C. G., Ed.; Elsevier: Amsterdam, 1981; p 273.

(7) (a) Mendes, E.; Oda, R.; Manohar, C.; Narayanan, J. *J. Phys. Chem. B* **1998**, *102*, 338−343. (b) Buwalda, R. T.; Stuart, M. C. A.; Engberts, J. B. F. N. *Langmuir* **2000**, *16*, 6780−6786. (c) Hassan, P. A.; Valaulikar, B. S.; Manohar, C.; Kern, F.; Bourdieu, L.; Candau, S. J. *Langmuir* **1996**, *12*, 4350−4357. (d) Narayanan, J.; Mendes, E.; Manohar, C. *Int. J. Mod. Phys. B* **2002**, *16*, 375−382.

(8) Wanka, G.; Hoffmann, H.; Ulbricht, W. *Colloid Polym. Sci.* **1990**, *268*, 101−117.

(9) Hoffmann, H.; Horbaschek, K.; Witte, F. *J. Colloid Interface Sci.* **2001**, *235*, 33−45.

(10) Majhi, P. R.; Blume, A. *J. Phys. Chem. B* **2002**, *106*, 10753−10763.

(11) Yin, H. Q.; Zhou, Z. K.; Huang, J. B.; Zheng, R.; Zhang, Y. Y. *Angew. Chem., Int. Ed.* **2003**, *42*, 2188−2191.

(12) (a) Zana, R. *In Surfactant Solutions. New Methods of Investigation;* Zana, R., Ed.; M. Dekker Inc.: New York, 1987; Chapter 5. (b) Miller, D. D.; Magid, L. J.; Evans, D. F. *J. Phys. Chem.* **1990**, *94*, 5921−5930. (c) Gehlen, M.; De Schryver, F. C. *Chem. Rev.* **1993**, *93*, 199.

(13) (a) Li, F.; Rosen, M. J.; Sulthana, S. B. *Langmuir* **2002**, *17*, 1037−1042. (b) Zhao, G. X.; Ding, F. X.; Zhu, B. Y. *Colloids Surf., A* **1998**, *132*, 1. (c) Siddiqui, F. A.; Franses, E. I. *Langmuir* **1996**, *12*, 354−362. (d) Zhou, Q.; Rosen, M. J. *Langmuir* **2003**, *19*, 4555−4562.

(14) (a) Bruinsma, R.; Gelbart, W.; Shaul, A. B. *J. Chem. Phys.* **1992**, *96*, 7710−7727. (b) Wang, S. Q. *J. Phys. Chem.* **1990**, *94*, 8381−8348. (c) Hofmann, S.; Hoffmann, H. *J. Phys. Chem. B* **1998**, *102*, 5614−5624. (d) Oelschlaeger, Cl.; Waton, G.; Candau, S. J.; Cates, M. E. *Langmuir* **2002**, *18*, 7265−7271.

(15) Lianos, P.; Lang, J.; Strazlelle, C.; Zana, R. *J. Phys. Chem.* **1982**, *86*, 1019−1025.

(16) (a) Israelachvili, J. N.; Mitchell, D. J.; Ninham, B. W. *J. Chem. Soc., Faraday Trans. 2* **1976**, *72*, 1525. (b) Israelachvili, J. N.; Mitchell, D. J.; Ninham, B. W. *Biochim. Biophys. Acta* **1977**, *470*, 185. (c) Israelachvili, J. N.; Marcelja, S.; Horn, R. G. Q. *Rev. Biophys.* **1980**, *13*, 121.

(17) (a) Nagarajan, R. *Structure-Performance Relationships in Surfactants*; Esumi, K., Ueno, M., Eds.; Marcel Dekker: New York, 1997; Chapter 1, pp 1−89. (b) Dill, K. A.; Flory, P. J. *Proc. Natl. Acad. Sci. U.S.A.* **1980**, *77*, 3115. (c) Ben-Shaul, A.; Szleifer, I.; Gelbart, W. M. *Proc. Natl. Acad. Sci. U.S.A.* **1984**, *81*, 4601. (d) Puvvada, S.; Blankschtein, D. *J. Phys. Chem.* **1992**, *96*, 5567−5579.

(18) (a) Kumar, S.; Sharma, D.; Din, K. U. *Langmuir* **2000**, *16*, 6821−6824. (b) Yu, Z. J.; Neuman, R. D. *Langmuir* **1994**, *10*, 377−380. (c) Yu, Z. J.; Xu, G. Z. *J. Phys. Chem.* **1989**, *93*, 7441−7445. (d) Srinivasa, R. R.; Hakan, E.; Kaler, E. W. *Langmuir* **2002**, *18*, 1056−1064. (e) Bales, B. L.; Zana, R. *Langmuir* **2004**, *20*, 1579−1581.

(19) (a) Brasher, L. L.; Herrington, K. L.; Kaler, E. W. *Langmuir* **1995**, *11*, 4267−4277. (b) Yin, H. Q.; Mao, M.; Huang, J. B.; Fu, H. L. *Langmuir* **2002**, *18*, 9198−9203.

(20) (a) Hoffmann, H.; Ebert, G. *Angew. Chem., Int. Ed. Engl.* **1988**, *27*, 2−912. (b) Amaral, L. Q.; Santin Filho, O.; Taddei, G.; Vila-Romeu, N. *Langmuir* **1997**, *13*, 5016−5021. (c) Filho, O. S.; Itri, R.; Amaral, L. Q. *J. Phys. Chem. B* **2000**, *104*, 959−964. (d) Oda, R.; Bourdieu, L. *J. Phys. Chem. B* **1997**, *101*, 5913−5916.

(21) Fenandez, Y. D.; Calvo, S. R.; Gramatges, A. P. *Phys. Chem. Chem. Phys.* **2002**, *4*, 5004−5006.